

The dynamical behaviour of the lifted temperature minimum^(*)

S. RAGOTHAMAN⁽¹⁾, R. NARASIMHA⁽²⁾^(**) and A. S. VASUDEVA MURTHY⁽³⁾

⁽¹⁾ *Department of Earth Sciences, Meteorology - Uppsala University, Uppsala, Sweden*

⁽²⁾ *Jawaharlal Nehru Centre for Advanced Scientific Research - Bangalore, India*

⁽³⁾ *TIFR Centre, Indian Institute of Science Campus - Bangalore 560012, India*

(ricevuto il 13 Gennaio 2000; revisionato il 5 Dicembre 2000; approvato il 20 Dicembre 2000)

Summary. — This paper concerns a phenomenon called the Ramdas Paradox by Lettau, referring to the occurrence of a minimum in the temperature some decimetres above ground on calm clear nights. Recently, Vasudeva Murthy, Srinivasan and Narasimha have proposed a theory that successfully reproduces the observed minima. We extend that work here to investigate the time evolution of near-ground temperature distributions through numerical simulations. It is demonstrated that, if the surface emissivity is not too close to unity, a lifted temperature minimum can appear shortly after sunset, but its subsequent evolution, depending strongly on ground cooling rate, can lead to i) monotonic growth, ii) near-steady state, or iii) growth followed by collapse. Solutions of the model to an appropriately formulated “turbulent transport episode” reveal that the lifted temperature minimum disappears after the commencement and reappears after the cessation of the gust in times of order 10–20 s, in qualitative agreement with the observations of Raschke. However, full recovery to the no-gust state takes times of order 10^3 s after the episode. This behaviour is identified with a two-time response of the cold layer, involving a quick radiative adjustment followed by a slow diffusive relaxation. It is concluded that the VSN model fully reproduces the observed dynamical behaviour of the lifted temperature minimum, and provides a satisfactory basis for the study of the near-ground thermal environment.

PACS 92.60.Fm – Boundary layer structure and processes.

PACS 47.70 – Reactive, radiative, or nonequilibrium flows.

1. – Introduction

An understanding of the nocturnal distribution of air temperature near ground is important for several reasons. First of all it affects different aspects of agricultural mete-

^(*) The authors of this paper have agreed to not receive the proofs for correction.

^(**) Also at the National Institute of Advanced Studies, Indian Institute of Science Campus, Bangalore 560 012, India. E-mail: roddam@caos.iisc.ernet.in

orology such as the formation of frost and fog and influences the dispersion of pollutants in the atmosphere. A clear insight into the physics underlying the subject seems essential to unravel the dynamical aspects of the stable nocturnal boundary layer, which is not yet well understood (*e.g.*, [5]). Finally, the relation between temperature right at the surface and the air temperature at screen or model level can significantly affect infrared global radiant flux estimates, as Garratt [6] has recently shown.

As part of an overall attack on this complex of problems, this paper deals with one specific aspect of it, namely the singular air temperature distribution that prevails above bare soil during calm, clear nights, first reported by Ramdas and Atmanathan [2]; a companion paper will discuss nocturnal inversions using the present approach. The phenomenon studied here is characterized by the emergence, next to ground, of a thin layer (typically less than 0.5 m) within which the air is cooler than ground by several degrees. (It is thus possible for air at plant level to reach freezing temperatures when both ground and screen-level temperatures are well above freezing.) Early reports of such a layer were treated with scepticism for many years (see, *e.g.*, [7]) for a variety of reasons, but in particular because such a cold layer appears to defy the Rayleigh criterion for convective instability. There is however overwhelming observational evidence now in favour of the lifted temperature minimum [4,8-10]. Lettau [1] has called the phenomenon the Ramdas Paradox. The history of early studies of the problem has been traced by Narasimha [11].

A sound theory for the phenomenon had till recently not been available. The only quantitative treatment of the problem was that of Zdunkowski [12], who invoked the presence of haze (not reported in many of the observational studies). The position regarding a convincing explanation of the Ramdas minimum had thus remained substantially the same as in the very interesting discussion that took place in the Royal Meteorological Society following the appearance of Lake's study. During this discussion (see [13]), Scorer asked, "Could the radiation experts tell us what they can and cannot explain with realistic models?", and Sutcliffe said he "would like to see differential equations set up in order to discuss whether values can be given to the parameters to permit the observed profiles to occur". This is precisely what [3] (Vasudeva Murthy, Srinivasan and Narasimha, to be referred to as VSN below) have done, by proposing a self-consistent theory for the "lifted temperature minimum" (as they call it) that appears to be in general accord with reported observations. Contrary to earlier proposed explanations (*e.g.*, [12]) the VSN theory shows that a careful modelling of the radiative transfer near ground, allowing the surface to have an emissivity ϵ_g less than unity, can reproduce the Ramdas minimum if the ground does not cool too rapidly. The important role played by radiation in energy transport near ground, especially at night, has been realized for a long time; *e.g.*, Geiger [7] cites studies by Falckenberg and his pupils during 1927-1936. In their first report, Ramdas and Atmanathan [2] also mention the role of radiation. However, radiative transfer near ground is a delicate balance, as Narasimha and Vasudeva Murthy [14] have shown; without accurate models it can be difficult to obtain the correct quantitative estimates of the different constituents of the budget. It is in principle necessary to include heat conduction within the soil in a complete theory, but VSN were able to demonstrate (by solving the full coupled soil-air problem) that a specified ground cooling rate produced equivalent predictions and made physical interpretation of the phenomenon easier.

The physical basis of the theory has been discussed at considerable length in VSN and Narasimha [11,15], but it may be worthwhile to provide a short summary here. The VSN model is based on the flux emissivity scheme for estimating radiative transfer in the atmosphere (*e.g.*, [16]). The first point to note is that, according to this scheme, the

radiative cooling of air near the ground depends chiefly on the product

$$(1 - \epsilon_g)d\epsilon_a/dz,$$

where ϵ_g is the emissivity of the ground and ϵ_a is the flux emissivity of (humid) air at height z above ground. The derivative of ϵ_a is very large near the ground $z = 0$, chiefly because of the strong absorption of infra-red radiation in the vibration-rotation bands of the water vapour molecule; this variation, which takes place in what VSN call the emissivity sublayer, has a characteristic length which is of the order of 1 m at a specific humidity of 0.01. Thus, even if the ground is nearly black radiatively, the cooling near ground can be substantial as long as $\epsilon_g \neq 1$. However, as the absorption is weak in other bands, especially the so-called atmospheric window over the 8–14 μm wavelength range, there is usually a radiative slip at ground; *i.e.* the temperature of air next to ground is different from that *at* ground. The sign of this slip is such that the ground is warmer if the soil is sufficiently conducting to keep surface cooling slow. Thermal diffusion in air—chiefly only molecular under calm conditions—smears out this slip into the cold layer that Ramdas observed.

Although attention is focussed here on the lifted minimum, it must be emphasised that the value of the study is not limited to such singular temperature distributions; on the other hand, the formulation of a successful model for energy transfer near ground has implications for many other phenomena connected with the nocturnal boundary layer, which we propose to explore in other publications. That the energy balance near ground is delicate and needs careful handling has been demonstrated by Narasimha and Vasudeva Murthy [14].

The theory underlying VSN highlights the role of ground emissivity and cooling rate in the emergence of a lifted minimum. However, while VSN provided maps in the surface emissivity/ground cooling rate plane that displayed the region in parameter space where a lifted minimum would occur some two hours after sunset, they did not touch on the question of how the temperature distribution near ground evolves during night. As we shall describe in the next section, there are several interesting fundamental questions concerning the *dynamics* of the lifted minimum. It is the purpose of this paper to describe the results of a series of numerical simulations we have conducted using the VSN model that shed light on this question.

A typical distribution containing a lifted minimum is shown in fig. 1. In studying its evolution, it is often sufficient to focus attention on two parameters that characterize the phenomenon, namely the location of the minimum z_{\min} and its intensity $\Delta T_{\min}(= T_g(t) - T(z_{\min}, t))$, where T_g denotes the ground temperature and $T(z, t)$ is the air temperature at height z and time t . To the extent that the profiles of T are roughly similar between $z = 0$ and z_{\min} , these two parameters provide an excellent summary of the chief characteristics of the evolution of $T(z, t)$.

2. – Evolution or steady state?

Before we proceed to report the results of the present study, it is useful to review the observational evidence on whether the temperature distribution near ground attains a steady state during night or not.

Now a diagram presented by Ramdas [17] appears to suggest that the height of the lifted minimum, as measured by him at a site in Pune (India), is almost constant—at about 30 cm—throughout the night, beginning about an hour after sunset (1800 hrs).

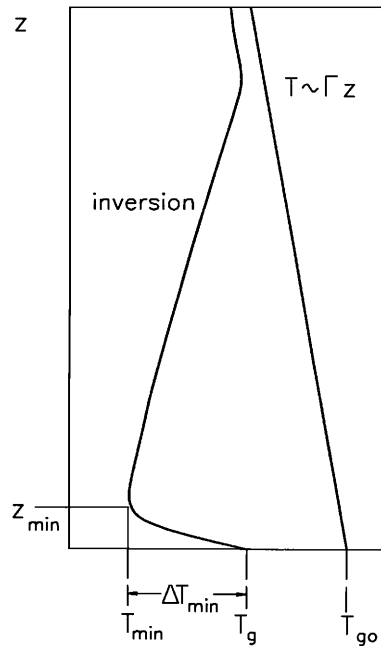


Fig. 1. – Schematic of the lifted temperature minimum.

However, a careful examination of the instrumentation used by Ramdas reveals that any change in the location of the minimum in the range 30–60 cm above ground would not have been detected, as no thermometers or probes were located in this range; thus, the table of data presented by Ramanathan and Ramdas [18] contains no readings between these two heights. Hence, we cannot conclude from these observations that the lifted minimum actually remained at the same height throughout the night; but it must have remained between 30 and 60 cm, and any evolution that might have taken place must have been very slow. Incidentally, there is no discussion by Ramdas [17] of surface properties at the site, which from the results of VSN, and those to be reported here, are crucial for the formation and evolution of the lifted minimum.

On the other hand, some kind of evolution is implicit in the observations of Raschke [4], who reports that, at his site (also in Pune but different from that of Ramdas), the lowest temperature was almost always recorded by the thermocouple at 10 cm height, but that in the early morning hours the values measured at a height of 1 cm were the lowest. This indicates that the height of the minimum, after reaching a maximum value, began to *decrease* late during night at his site. A similar behaviour is reported for the temperature differential ΔT_{\min} also.

Lake [13] does not present any quantitative account of the evolution of the location of the lifted minimum, but his observation that “the negative difference between the surface temperature and that at any height up to 54 in increased with time as long as the conditions remained stable” does indicate some evolution, and it is very likely that a similar conclusion should be valid for ΔT_{\min} also.

Oke [10] reports that with clear skies and winds $< 1 \text{ ms}^{-1}$, the usual lifted minimum profile was observed; on some occasions z_{\min} was as high as 50 cm and ΔT_{\min}

often exceeded 3°C. However, his measurements were not made during completely calm conditions, as shown by table 1 of his paper. They therefore do not provide any direct evidence on the question of evolution under calm conditions, but do indicate that whenever windspeed increased, z_{\min} decreased.

In this context, it should be noted that the nocturnal boundary layer itself has been shown to be evolving in several studies (*e.g.*, [19, 20]), and hence it has been argued that its structure cannot be studied using steady-state formulations. Kuo [21] and Kondo [22] also find that steady-state conditions cannot be assumed to prevail in the atmosphere during night. Although proponents of quasi-steady state formulations are not lacking (see, *e.g.* [23]), it now seems clear that the boundary layer is in general not in a steady state during night. These points, considered together with the fact that the ground itself is cooling continuously during night, would suggest that the lifted minimum itself should in general evolve during night. In the light of this discussion, it is clear that the question of evolution remains to be studied thoroughly.

Paradoxically, however, there is a related intriguing observation reported by Raschke [4] that suggests that the temperature distribution responds extremely rapidly to certain perturbations. Thus, when a sheet of plywood was waved in the neighbourhood of his instrumentation, Raschke found that the lifted minimum that had prevailed till then was immediately destroyed, only to reappear in less than a minute after the waving was stopped. Although it is now well understood why it would not take much turbulent diffusion to destroy the lifted minimum (VSN), it has not been clear what mechanism governs the quick reemergence noted by Raschke. A study of the dynamics of the phenomenon would therefore be incomplete without an examination of the response of the lifted minimum to a turbulence perturbation, and of the time constants that govern the physics of the phenomenon in the light of the VSN model. It is particularly important to see how the time constants proposed therein are related to the aforementioned response.

In sect. 3, we briefly present the VSN model and the parametrisation of turbulence that we shall adopt, and the salient features of the numerical methodology used to solve the governing equation. The results of the simulation are presented in sect. 4 and 5 and a concluding discussion is offered in sect. 6.

3. – Problem formulation and method of solution

As the model used here has already been presented in detail, we restrict ourselves to a brief description.

3.1. The VSN model. – The model considers clear nights with no advective changes. Wind profile, soil temperature variation and the humidity of the air are incorporated into the model as parameters that can be prescribed; although the soil temperature can be independently computed through a coupled air-soil model, also formulated in VSN, we shall restrict ourselves to the approach where the ground temperature is a prescribed function of time, as this has been shown to be entirely adequate and furthermore has the advantage of providing a more immediate physical interpretation. Horizontal homogeneity is also assumed, so that the air temperature T is a function only of vertical distance z from the ground surface and time t . The governing equation for the problem, which is based on energy balance, can then be written as

$$(1) \quad \rho_a c_p \frac{\partial T}{\partial t} = - \frac{\partial Q}{\partial z},$$

where ρ_a is the density of air, c_p is the specific heat at constant pressure and Q is the total energy flux, split into three components,

$$(2) \quad Q = Q_m + Q_t + Q_r,$$

where Q_m , Q_t and Q_r are the contributions to the energy flux from conduction, convection and long-wave radiation, respectively. The first two terms are given by

$$(3) \quad Q_m = -k_m \frac{\partial T}{\partial z}, \quad Q_t = -k_t \frac{\partial \theta}{\partial z}, \quad \theta = T + \Gamma z,$$

where k_m is the molecular conductivity of air, k_t is the eddy conductivity, θ is the potential temperature and Γ is a (prescribed) constant lapse rate. There are today a variety of sophisticated models that seek to provide estimates of turbulent transport in general and the eddy conductivity in particular (see, *e.g.*, [5]). However, as both theory and observation indicate that the lifted temperature minimum disappears in the presence of modest turbulent transport, it is wasteful for our present purpose to adopt any of these sophisticated models. Instead, an algebraic expression for k_t should suffice. We thus assume the eddy conductivity to be given by the expression

$$(4) \quad k_t = \rho_a c_p U_* k_* z \phi(\text{Ri}),$$

where U_* is the friction velocity, k_* is the Karman constant and $\phi(\text{Ri})$ is a stability function. Here again there are many proposals, but one we have found both convenient and appropriate, and consistent with the observational data of Businger *et al.* [24], is a fairly widely used expression from Liou and Ou [25],

$$(5) \quad \begin{aligned} \phi(\text{Ri}) &= 1.35(1 - 9\text{Ri})^{-1/2} && \text{for } \text{Ri} \leq 0, \\ &= 1.35(1 + 6.35\text{Ri})^{-1} && \text{for } \text{Ri} > 0, \end{aligned}$$

Ri being the Richardson number

$$(6) \quad \text{Ri} = \frac{k_*^2 g z^2}{U_*^2 \theta} \frac{\partial \theta}{\partial z}.$$

The molecular and eddy diffusivities are given by

$$K_m = k_m / \rho_a c_p, \quad K_t = k_t / \rho_a c_p.$$

In the study by VSN, the convection term was included chiefly to assess the role of turbulence in the phenomenon and to account for any residual turbulence left in the atmosphere. In the present study, apart from these reasons, the convection term is needed mainly for the study of the response of the lifted minimum to a rapid increase in eddy diffusion during a short gust, or more precisely a turbulence episode. VSN discuss in some detail the reasons behind the choice of this particular way of modelling Q_t .

The radiative flux Q_r is given by

$$(7) \quad Q_r = F^\uparrow - F^\downarrow,$$

where F^\uparrow and F^\downarrow are the upward and downward radiative fluxes, respectively. They are modelled here using a slight modification of the broadband flux emissivity method (as described, *e.g.*, by Liou [16] and Liou and Ou [25]). We thus take

$$(8) \quad F^\downarrow = \int_u^{u_\infty} \sigma T^4(u', t) \frac{d\epsilon}{du'} (u' - u) du',$$

$$(9) \quad F^\uparrow = \{\epsilon_g \sigma T_g^4(t) + (1 - \epsilon_g) F^\downarrow(0)\} \{1 - \epsilon(u)\} - \int_0^u \sigma T^4(u', t) \frac{d\epsilon}{du'} (u - u') du',$$

where u is the water vapour mass path length, given by

$$(10) \quad u(z) = \int_0^z \rho_w(z') \left\{ \frac{p(z')}{p(0)} \right\}^\delta dz',$$

$\rho_w(z)$ denotes the density of water vapour at level z , $p(z)$ denotes the pressure of air at level z and $u_\infty = u(\infty)$ is the total atmospheric path length. The exponent δ is chosen to be 0.9, following Garratt and Brost [26]. ϵ_g is the ground emissivity, σ is the Stefan-Boltzmann constant, $T_g(t)$ is the ground temperature and $\epsilon(u)$ is the broadband flux emissivity function of water vapour, which is taken here as

$$(11) \quad \begin{aligned} \epsilon(u) &= 0.0492 \ln(1 + 1263.5u) && \text{for } u \leq 10^{-2} \text{ kg m}^{-2}, \\ &= 0.05624 \ln(1 + 875u) && \text{for } u > 10^{-2} \text{ kg m}^{-2}, \end{aligned}$$

following Zdunkowski and Johnson [27].

Usually, eq. (9) for the upflux is written assuming $\epsilon_g = 1$. However it is being increasingly realized that it is important in many situations to allow for a gray surface with $\epsilon_g \neq 1$, and we have incorporated the appropriate modification following Paltridge and Platt [28]; see also Garratt and Brost [26].

Actually there are conditions when the effect of carbon dioxide on the absorption and emission of long-wave radiation may also be of some importance. This effect can be included by devising a more general prescription of the flux emissivity in terms of a composite optical path variable. However, this introduces inessential complexity into the problem, which we have judged to be not justifiable at the present stage of investigation.

The boundary conditions are taken to be

$$(12) \quad T(z, 0) = T_{g0} - \Gamma z,$$

$$(13) \quad T(0, t) = T_{g0} - \beta \sqrt{t},$$

$$(14) \quad \frac{\partial T}{\partial z}(\infty, t) = -\Gamma,$$

where β is the ground cooling rate parameter. The form (13) for the ground temperature is based on the well-known work of Brunt [29], who showed that β is inversely proportional to the square root of the thermal diffusivity of the soil. The initial condition (12) is nominally prescribed at sunset although it becomes realistic only after a short transient around the time of sunset. However, it must be appreciated that the solar radiant energy flux received at the ground (per unit surface area) starts diminishing rather before sunset.

Correspondingly there is an evening transitional epoch over which the solutions computed here cannot be expected to be strictly valid. However, boundary layer studies suggest that the transitional epoch can be surprisingly short (*e.g.*, [30]). Thus, although the instantaneous initial condition we have imposed is not strictly achieved in the atmosphere, we expect it to be realistic shortly after sunset. We shall find it convenient to refer to $t = 0$ as the time of “nominal sunset”.

3'2. Parameterisation of “turbulence episode”. – Before we proceed to describe how we propose to analyse the effect of a wind perturbation through the present model, it is worthwhile to discuss the motivation for undertaking such a study.

A remarkable finding in Raschke’s observations was the rapidity with which the lifted minimum could be destroyed or restored depending on wind. It is first of all necessary to recall that his observations were made on the remarkably flat plateau of Chaturshringi Hill in Pune—a site at which advection could be ruled out. This was confirmed by the fact that when wind velocity *dropped*, air at a height of 1 cm cooled more intensely than at 1 mm above ground. When a temperature minimum occurred above ground, the wind velocity measured at a height of 20 cm always remained below 0.5 ms^{-1} . If wind velocity fell below this critical value, then the air layers near the ground cooled within a few minutes relative to the soil surface and the temperature minimum moved up in height. When the wind velocity increased, a sudden temperature increase was recorded only by the lower thermographs showing that the advection of warm air could not have been the cause. Indeed, it was found that the temperature distribution would be influenced, even at a given (low) mean wind, if the *fluctuations* were strong enough (see [4], fig. 11). Finally it was found that vigorous waving of a plywood sheet in the neighbourhood could reverse the temperature distribution and destroy the lifted minimum; but when the waving ceased “the minimum at 10 cm height above the ground was recovered in less than 1 min.” (All quotes from Raschke here are taken from its English translation, available as Report 94 AS 2 from the authors.)

Based on these observations, Raschke concludes that “it is actually not the wind velocity but the prevailing eddy transport which determines the form of the temperature profile”. He therefore proposes that the temperature profile “depends on the wind velocity only indirectly through the exchange coefficient”.

One of our objectives in the present investigation is to understand the mechanism underlying the rapid response to what it is convenient to call a “turbulence episode” of the kind that Raschke so carefully investigated. It is of course hopeless to try and simulate in any precise way the wind disturbances that actually occurred, or were created by waving plywood sheets, if only because there is no further data on them. On the other hand, it strains the imagination to think that such precise simulation is necessary to elucidate the *physics* of the phenomenon. Once advection is ruled out, and it is seen that eddy diffusion is the main factor, two ways of simulating such an episode suggest themselves.

- i) We can artificially increase the molecular diffusivity by a certain factor, if necessary within a certain height and during a prescribed interval. This is somewhat similar to the exercises carried out by Zdunkowski [12] to simulate turbulence.
- ii) Recalling that in the VSN model the eddy diffusivity is proportional to the friction velocity U^* , we can increase U^* over a short period of time.

Following method i) is open to the objection that it is entirely artificial, introduces several new parameters into the problem, and takes no account of the stability of the

flow in the conditions being investigated. Method ii) at first also appears artificial, as in principle the whole boundary layer profile is altered over a short period whose duration is less than the order of the boundary layer time constant, and so an eddy diffusivity that is strictly valid only in equilibrium is used for describing a short-duration episode.

Note that, in the advection-less 1D model we are using, the wind itself is not important, only the eddy diffusion it produces, in accordance with Raschke's conclusions. To this extent, therefore, we may look upon the increase in U^* as just mimicking the increase in diffusion characteristic of the eddy episode. This procedure has the additional advantage of taking account of the effects of height above ground and stability in some way. It cannot, and is not intended to, simulate a true gust episode; we see no simple way of doing it, in any case. It should however be adequate to throw light on the *physics* underlying the rapid changes that the layer next to ground so dramatically displays, in response to sudden changes in eddy transport. Using a continuous analytical expression has the advantage that no artificial kinks are introduced into the solution, at the points where, *e.g.*, the diffusivity is cut off or changed to a different value; in our previous experience with these simulations, the results have been found to be sensitive to such discontinuities.

We may therefore model the episode by prescribing a friction velocity at the relatively high value of 1 ms^{-1} during the episode and switching it off to zero during calm periods. We will, for convenience, term such an episode a "gust", fully aware that a real gust is too local in time and space to be represented by a change in U_* . The duration of the gust is taken to be 30 seconds, as preliminary studies showed that this is long enough to destroy the most intense lifted minimum encountered in the present investigation, which incidentally occurs in a simulation of the effect of a very high molecular conductivity (ten times the value for air). Thus the friction velocity assumes a top hat profile in the numerical experiments carried out here, U_* being zero till 1 h after nominal sunset, the gust being then turned on with $U_* = 1 \text{ ms}^{-1}$, and turned off 30 s later.

3.3. Numerical methodology. – The basic approach for solving the governing equation is based on the method of lines, with eq. (1) discretized in two stages. In the first stage, the space variable is discretized on a selected space mesh chosen *a priori* for the entire calculation, so as to convert (1) into a system of ordinary differential equations with time as the independent variable. This system is then solved using a standard software package with an appropriate discretization in time, to be discussed below. This approach is essentially the same as VSN have adopted in their earlier study [31], where more details can be found.

Following several exploratory studies to determine the optimum spatial discretization, the whole domain is divided first into a fixed number of slabs (four in the present case; 0 to 2 m, 2 m to 20 m, 20 m to 200 m and 200 m to 1 km). Note that the slabs are of unequal height, because of the wide disparity in scales involved in the problem. Within each slab, a uniform mesh is chosen, namely 500 points between ground and 2 m, 100 between 2 m and 20 m, 150 between 20 m and 200 m and 250 between 200 m and 1 km, making a total of 1000 points in the whole domain.

The code sets its own time step between prescribed limits, depending on specified tolerance on the solution. In simulations of the turbulence episode, temperature profiles up to 1 h are computed with $U_* = 0$. Then the profile at 1 h is prescribed as the initial condition to compute the temperatures for the next 30 s with $U_* = 1 \text{ ms}^{-1}$. Finally, the profile at 1 h 30 s is prescribed as the initial profile to compute temperatures from 1 h 30 s up to 12 h, with $U_* = 0$. This procedure is necessary to ensure that the code

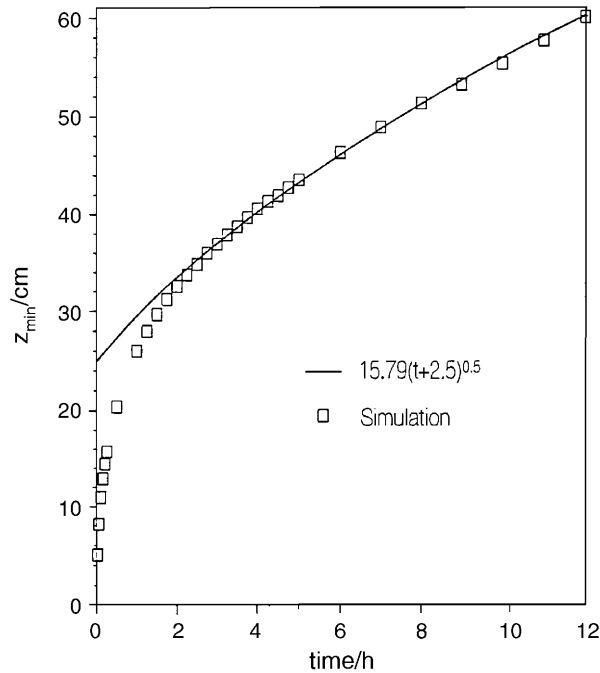


Fig. 2. – Complete evolution of the height of the lifted minimum for the baseline case; $\epsilon_g = 0.8$ and $\beta = 2 \text{ Kh}^{-1/2}$.

resolves the evolution during the turbulence episode properly. As soon as U_* is turned on there is a rapid variation of temperature, to capture which the time step needs to be very small. It was found from the computations that, during the turbulence episode, the time step chosen automatically by the code is sometimes as small as 0.15 s, for the specified tolerance of 10^{-4} K, in all the computations reported here. The solutions are stable, with no evidence of any oscillations.

4. – Evolution of lifted minimum under calm clear conditions

To gain insights into the evolution of the temperature distribution, it is unnecessary to examine all the profiles, as they tend to be roughly similar in shape from ground to the temperature minimum. It is therefore sufficient to focus on the location of the lifted minimum z_{\min} and the temperature differential ΔT_{\min} . The value of z_{\min} is determined as the lowest height at which the temperature gradient vanishes (the position being estimated, in cases where the temperature profile is flat, by making least-squares fits to sets of 5 computed points in z on either side of this height). We shall first describe the evolution of z_{\min} , and later that of the intensity of the lifted minimum, for different values of the parameters ϵ_g and β .

4.1. Evolution of z_{\min} . – It is convenient to take the conditions $\epsilon_g = 0.8$ and $\beta = 2 \text{ Kh}^{-1/2}$ as constituting a “baseline” case, following the choice made by Narasimha and Vasudeva Murthy [14]. Figure 2 shows the evolution of z_{\min} for this case. It can be seen that z_{\min} begins to increase in proportion to \sqrt{t} about 3 hours after nominal sunset;

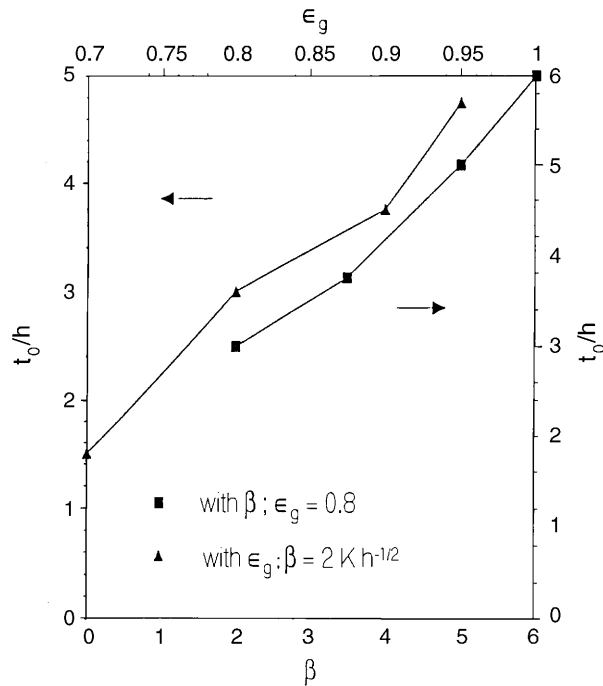


Fig. 3. – Variation of the time of on-set of the \sqrt{t} behaviour with ϵ_g and β .

the least-squares fit shown in fig. 2 was made for z_{\min} beyond this period. The r.m.s. deviation of the fit from the simulation result, as a fraction of the latter, is required to be less than 2% (in this as well as other fits made in this study).

Figure 3 shows the variation, with β , of the time t_0 from which \sqrt{t} behaviour is obeyed in the above sense. It can be seen that as the ground cools more rapidly (up to $\beta = 6 \text{ Kh}^{-1/2}$), the onset of \sqrt{t} behaviour is delayed. Figure 3 also shows the variation of t_0 with ϵ_g . In this case also, the \sqrt{t} behaviour sets in later for higher values of the ground emissivity.

Figure 4 shows the evolution of z_{\min} for very high values of β ($> 6 \text{ Kh}^{-1/2}$) and $\epsilon_g = 0.8$. It can be seen that, after reaching a maximum value, z_{\min} remains nearly constant for $\beta = 7$ and $7.5 \text{ Kh}^{-1/2}$. For the former case it becomes constant at $t = 10$ h, and for the latter at $t = 6$ h after nominal sunset. For $\beta > 7.5 \text{ Kh}^{-1/2}$, the location of the minimum, after reaching a maximum value, begins to decrease gradually as the lifted minimum evolves in time. For values of $\beta > 12 \text{ Kh}^{-1/2}$, the lifted minimum ceases to occur at any time.

It is immediately clear from this diagram that there are four regimes in the evolution of the Ramdas layer; it can grow, remain relatively steady, collapse or not occur at all depending on surface parameters. The conflicting observations recounted in sect. 2 could therefore have the simple explanation that they were in different (site-dependent) regimes.

The \sqrt{t} dependence of z_{\min} suggests immediately diffusive behaviour as in the analogous, thermal Rayleigh problem. This is the case of a flat plate whose temperature changes discontinuously at $t = 0$ to a value higher than the ambient [32]. The solution to

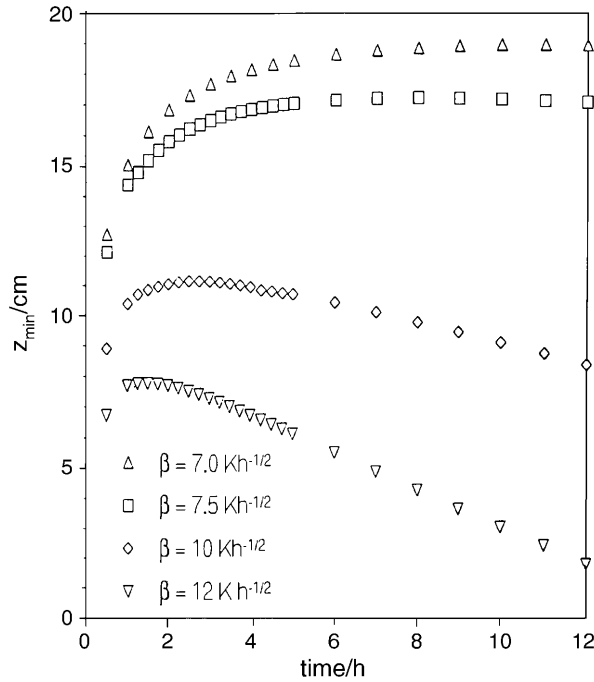


Fig. 4. – Evolution of the height of the lifted minimum for $\beta > 6 \text{ Kh}^{-1/2}$.

this problem contains a thermal boundary layer that grows in proportion to the square root of time. From the solutions presented in figs. 2 and 3, the analogy is clearly valid at times well after sunset for sufficiently low values of the ground cooling rate. The coefficient of \sqrt{t} in the fit shown in fig. 3 is approximately equal to $(0.3 K_m)^{1/2}$, *i.e.* the depth of the cold layer depends on the thermal diffusivity. This is consistent with the VSN theory, according to which the lifted minimum is caused by the smearing of the radiative slip in temperature (under an inversion) by molecular conduction.

However, it must be noted that unlike in the thermal Rayleigh problem, the boundary condition in the present problem is not steady, as the ground continues to cool throughout the night. The analogy thus breaks down for relatively high values of the ground cooling rate, indeed to such an extent that eventually the lifted minimum disappears altogether, as is also predicted by the maps given by VSN.

We shall now consider the short-time evolution of z_{\min} , which is also shown in fig. 2 for $\epsilon_g = 0.8$ and $\beta = 2.0 \text{ Kh}^{-1/2}$. It can be seen that z_{\min} increases rapidly during the first few minutes after nominal sunset and much more slowly at larger times; thus z_{\min} is already about 10 cm at $t = 6$ minutes and only 60 cm 12 hours later, and so reaches 1/6 of its maximum value during 1/120 of the total period of evolution. A similar rapid variation during the initial few minutes is observed for all values of ground emissivity and cooling rate which yield a lifted minimum. Hence we find that, irrespective of surface properties, the short-time evolution of z_{\min} is relatively rapid, but that this may be followed by either a slower increase, or if β is too high and/or ϵ_g too low, even a gradual decrease.

For the simulations discussed above, K_m was set equal to the standard value for air, namely $2.5 \times 10^{-5} \text{ m}^2 \text{ s}^{-1}$ ($=K_{m0}$, say). In order to verify that the dynamics of the layer is

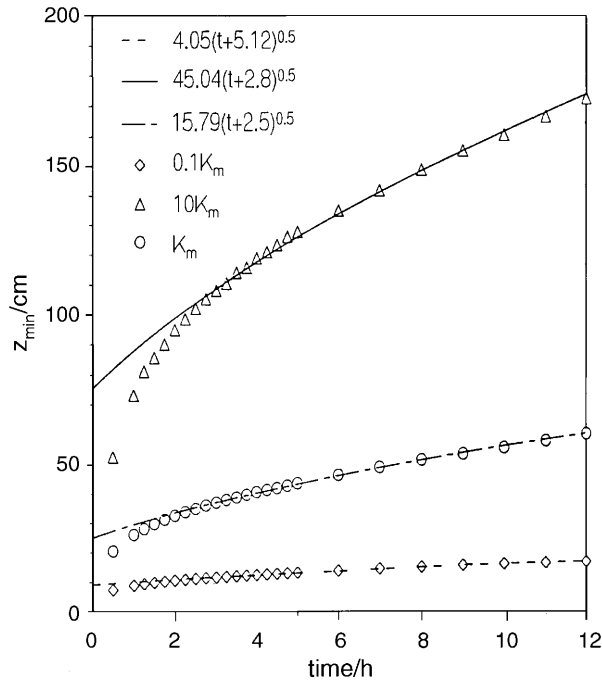


Fig. 5. – Evolution of the height of the lifted minimum for three different molecular diffusivities, 0.1, 1.0 and 10 times the standard value for air.

determined by conduction, simulations were performed with values of conductivity that were respectively 10 times higher and lower than the standard value for air. Figure 5 illustrates the evolution of z_{\min} for these values of K_m in the baseline case. It can be seen that the \sqrt{t} behaviour is observed here also, and as expected, z_{\min} is larger for a higher value of K_m confirming that thermal diffusion is the basic mechanism that balances radiative transfer in the layer.

4.2. Evolution of ΔT_{\min} . – We shall first consider the long time evolution (of the order of hours) of this parameter. Figure 6 shows that in the baseline case, ΔT_{\min} increases very slowly—roughly in proportion to $\log t$. Figure 6 also shows the same dependence when $\epsilon_g = 0.95$.

For values of β higher than $2 \text{ Kh}^{-1/2}$, the evolution is shown in fig. 7. It can be seen that for $\epsilon_g = 0.8$ and $\beta = 5 \text{ Kh}^{-1/2}$, the intensity of the minimum is almost constant at about 3.4 K right from about 4 h. For still higher values of β ($> 5 \text{ Kh}^{-1/2}$), ΔT_{\min} , after reaching a maximum value, begins to decrease. When $\beta = 12 \text{ Kh}^{-1/2}$, the intensity has become zero at 12 h.

Hence we find that, sufficiently long after sunset the intensity of the minimum increases roughly like $\log t$ for low values of the ground cooling rate, remains almost constant in time for β up to about $5 \text{ Kh}^{-1/2}$, and begins to decrease after reaching a maximum for still higher values of β ($> 7.5 \text{ Kh}^{-1/2}$), as the lifted minimum begins to weaken at these values of the ground cooling rate.

Let us now consider the short-time evolution of the intensity of the minimum, which is also shown in fig. 6. It can be seen that in the baseline case the intensity is 1.8 K at

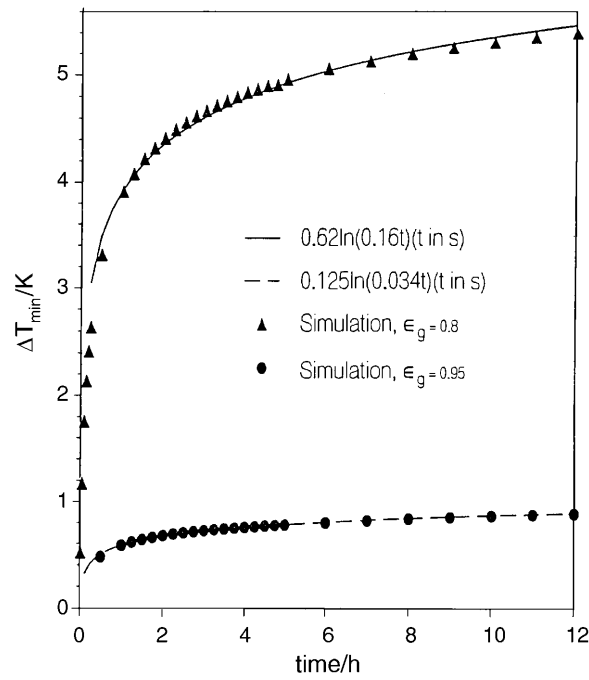


Fig. 6. – Evolution of the intensity of the lifted minimum for two cases; $\epsilon_g = 0.8$ and 0.95 with $\beta = 2 \text{ Kh}^{-1/2}$.

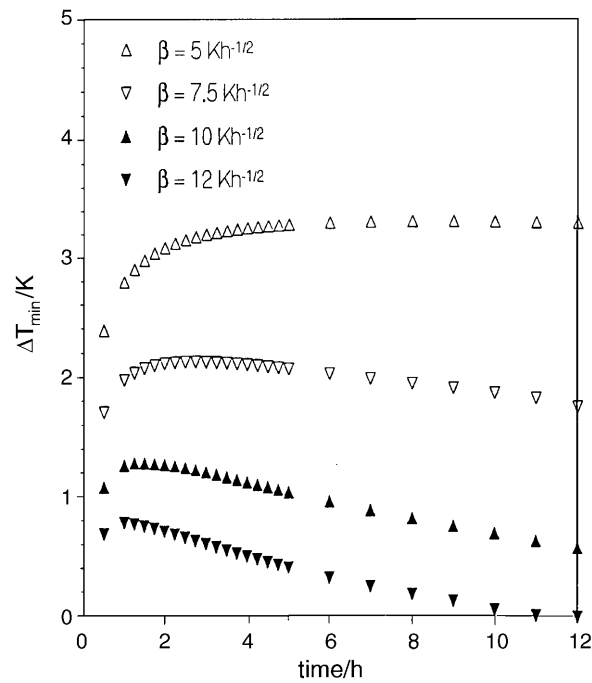


Fig. 7. – Evolution of the intensity of the lifted minimum for $\beta \geq 5 \text{ Kh}^{-1/2}$.

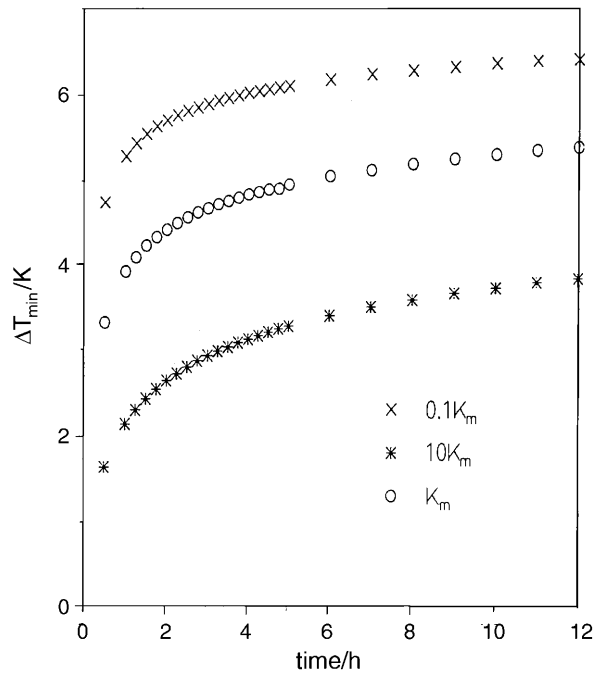


Fig. 8. – Evolution of the intensity of the minimum for three different molecular diffusivities, 0.1, 1.0 and 10 times the standard value for air.

6 minutes after nominal sunset and 5.4 K about 12 hours later. That is, ΔT_{\min} attains 1/3 of its maximum value in 1/120 of the total period of evolution. For other values of surface parameters that yield a lifted minimum also, this rapid variation in the first few minutes prevails.

Thus the behaviour of z_{\min} and ΔT_{\min} suggests that two disparate time scales are involved in the evolution of the lifted minimum. We shall return to this question in the next section.

Figure 8 illustrates the evolution of ΔT_{\min} for three different values of K_m . It can be seen that ΔT_{\min} decreases with increasing K_m ; higher diffusivity tends to smear out and reduce temperature differences. Hence, the observed variation of ΔT_{\min} with K_m confirms the picture of a conduction layer near ground.

4.3. Comparison with observations. – As will be seen from our review of observational evidence in sect. 2, the only results available for comparison with the present simulations are those of Ramdas [17].

For these simulations, we have taken

$$(15) \quad T_{g0} = 302.58 \text{ K}$$

as reported by Ramanathan and Ramdas [18]. However we do not have a value for β . We have carried out simulations for $\beta = 2 \text{ Kh}^{-1/2}$ and $\beta = 5 \text{ Kh}^{-1/2}$, and compare the results with Ramdas's observations in fig. 9a.

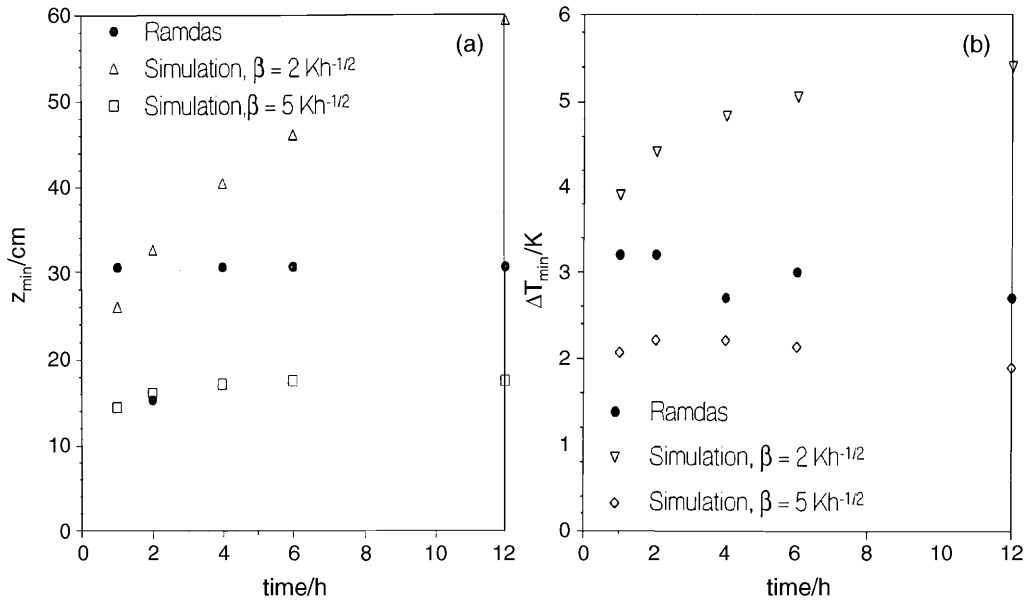


Fig. 9. – a) Comparison between observations of z_{\min} by Ramdas and the present simulation results for $\beta = 2$ and $5 \text{ Kh}^{-1/2}$ with $\epsilon_g = 0.8$. b) Same as a), but for ΔT_{\min} .

It is seen that the values of z_{\min} reported by Ramdas lie within the range of values of z_{\min} obtained by the present simulation for the two values of β . Also, as pointed out in sect. 2, there is the possibility that z_{\min} could have varied between 30 and 60 cm without being recorded, as there were no detectors within that height range. Figure 9b shows that the evolution of the intensity of the minimum, as observed by Ramdas, also lies within the range of values obtained from the present simulations. As the values of β and ϵ_g at the site of these measurements are not known, we can only conclude that the present theory is consistent with observations.

5. – Response to turbulence episode

We now turn to consider the response of the near-ground temperature distribution to the “gust” specified in subsect. 3.2. As we shall shortly see, this is strong enough to destroy the lifted minimum; we are particularly interested in the evolution of the temperature distribution after the cessation of the gust.

5.1. The nature of the response. – We once again consider the baseline case, $\epsilon_g = 0.8$ and $\beta = 2.0 \text{ Kh}^{-1/2}$. First we examine the effect of the gust on the lifted minimum and its short time evolution after the gust ceases. Figure 10a shows the temperature distributions during the 30-second gust, and fig. 10b those immediately after its withdrawal. It can be seen that, 20 s after the gust has commenced, the lifted minimum has disappeared; at this instant the temperature distribution is almost isothermal up to about a metre from the ground, and at greater heights—above 50 m (beyond the inversion)—it follows the prescribed lapse rate. This quick disappearance of the lifted minimum is consistent with the observation that it does not take much turbulent diffusion to destroy

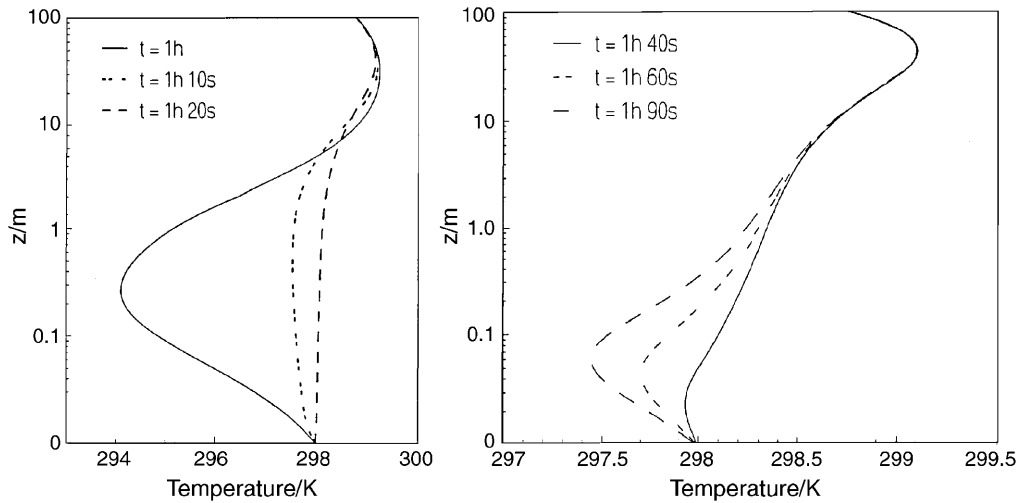


Fig. 10. – a) The temperature distribution up to 100 m before and during the gust, showing the disappearance of the lifted minimum. b) The temperature distribution up to 100 m after the cessation of the gust, showing the reemergence of the lifted minimum.

it (VSN). It can also be seen that after the gust is stopped at $t = 1 \text{ h } 30\text{s}$, the lifted minimum has already reappeared within 10 s; the reemergence is thus very rapid. This is in qualitative agreement with the observation by Raschke [4] of the response of the temperature distribution when he waved a sheet of plywood in the neighbourhood of his temperature sensors; he reports: “After the waving is stopped, the minimum at 10 cm height above the ground was again recovered in less than 1 min”, but the related graph (fig. 12 of his paper) indicates only the reemergence of the minimum, not its position. In our simulation, the minimum has an intensity of 3.4 K at 24 cm height before the gust commenced; one minute after the gust ceases, the intensity is only 0.53 K and the minimum occurs at 5.2 cm height. Thus, the lifted minimum quickly reappears but does not recover its pre-gust position immediately.

Furthermore, it is also seen from fig. 10a and b that both the location and the intensity of the lifted minimum are still evolving 60 s after the gust ceases. The further evolution of the lifted minimum at later times is illustrated in fig. 11 and compared with the no-gust baseline solution. It is seen that both z_{\min} (28 cm out of 32 cm) and ΔT_{\min} (4.1 K out of 4.4 K) are within 90 % of the baseline solution only 1 h after the gust is stopped. Thus, it takes a relatively long time—of the order of an hour—for the temperature distribution to approach the baseline solution, although a lifted minimum reappears very quickly after the gust is stopped.

Thus, when calm conditions are restored after the gust, there occurs a quick adjustment leading to the reemergence of the lifted minimum, followed by a much slower relaxation to the baseline solution. This reinforces the earlier suggestion (sect. 3) that two disparate time scales are involved in the response of the temperature distribution.

5.2. The quick adjustment. – In order to describe this process, we examine the temperature gradient at ground, *i.e.* $\partial T/\partial z|_{z=0}$, since this can define for us the time of re-formation of the lifted minimum accurately. Figure 12 shows the evolution of the tem-

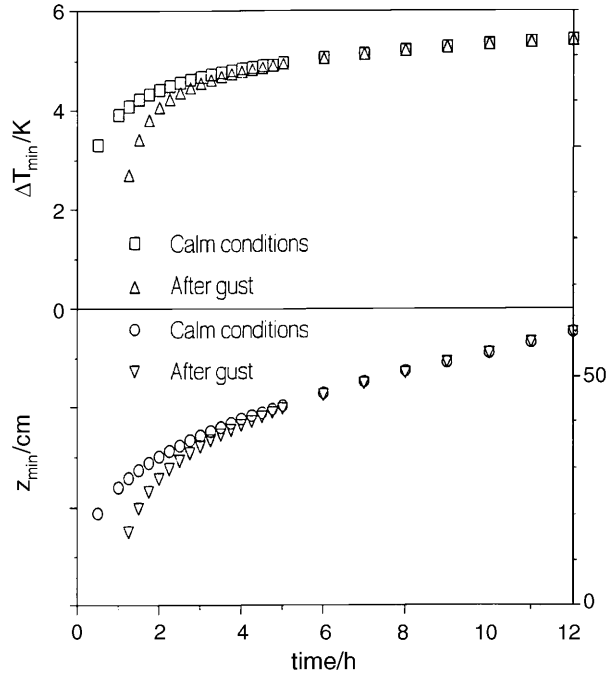


Fig. 11. – The approach to baseline of the lifted minimum as it recovers from the gust.

perature gradient at ground for the baseline case. It can be seen from fig. 12 that when the lifted minimum is yet to reappear, the temperature gradients at ground are positive, and indeed the temperature increases monotonically with height above the ground upto 50 m. When the lifted minimum has reappeared, the temperature gradients below the location of the minimum are negative for obvious reasons. Hence, changes in the sign of the gradient at ground provide an excellent indication of the presence or absence of the lifted minimum.

We can now define the time constant associated with the short-time response, denoted by τ_{fast} , as the time (after the gust ceases) at which the temperature gradient at ground $\partial T/\partial z|_{z=0}$ crosses zero on its way from a positive to a negative value. While there may be other ways of defining τ_{fast} , the present definition certainly determines the time of reappearance of the lifted minimum after the gust accurately and objectively.

The zero crossing in fig. 12 occurs at about 3.5 s, which is therefore the value of τ_{fast} as defined above. Let us now estimate, for the sake of comparison, the radiative time constants proposed by VSN. The first is given by

$$(16) \quad \tau_r = c_p \{ \sigma T_g^3 \epsilon'(0) \}^{-1}.$$

(This differs slightly from the VSN definition, which had T_{g0} in place of T_g . As the radiative time constants are very short, the ground temperature at the time of the gust is clearly more relevant.). Substituting appropriate values, it is found that τ_r is equal to 11 s.

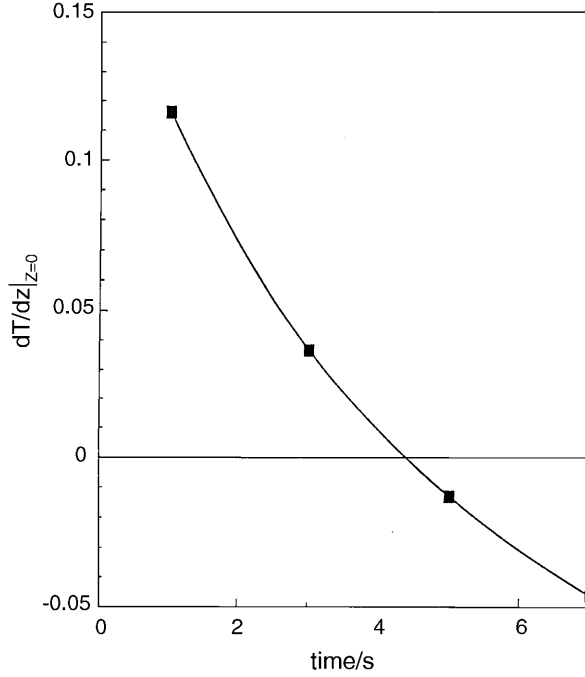


Fig. 12. – The evolution during the initial minutes (after gust) of the temperature gradient at ground for the baseline case; $\epsilon_g = 0.8$ and $\beta = 2 \text{ Kh}^{-1/2}$.

The second proposal is

$$(17) \quad \tau'_r = \frac{\tau_r}{(1 - \epsilon_g)(1 - \epsilon_\infty)},$$

where ϵ_∞ has been defined in sect. 3. It can be seen that τ'_r increases with ϵ_g , unlike τ_r which is independent of ϵ_g .

In order to find out the relation, if any, between these two estimates of the radiative time constant and τ_{fast} , several simulations have been run for different values of ϵ_g . The values of τ_{fast} from these simulations are listed in table I along with τ_r and τ'_r . It is seen that τ_{fast} increases with ϵ_g , like τ'_r , but that it is generally of the same order as τ_r . However, as the ground emissivity approaches unity, τ_{fast} increases towards the same order as τ'_r .

Further simulations with different values of K_m show that τ_{fast} is almost constant at about 4 s when K_m varies by a factor of 4, implying that the quick adjustment is not influenced by the thermal diffusivity.

5.3. Approach to baseline solution. – We now determine the time constant associated with the slow relaxation and the mechanism responsible. We determine this time constant, τ_{slow} , in terms of a quantity Dz_{min} , which is defined as

$$(18) \quad Dz_{\text{min}}(t) = \frac{z_{\text{min}}(t; \text{no gust}) - z_{\text{min}}(t; \text{after gust})}{z_{\text{min}}(t; \text{no gust})}.$$

TABLE I. – *The fast time constant in gust episode.*

ϵ_g	τ_r (s)	τ'_r (s)	τ_{fast} (s)
0.8	11	110	4
0.85	11	147	10
0.9	11	220	25
0.95	11	440	95

In the above relation, all quantities are evaluated at the same time t ; “no gust” in brackets denotes values under calm clear conditions and “after gust” denotes values during the evolution after the cessation of the gust. Clearly, Dz_{min} represents the departure from the baseline solution of the height of the lifted minimum due to the gust. From fig. 13, it can be seen that, as expected, the value of Dz_{min} decreases from a peak of 1 at $t = 1$ h 30 s to zero as the lifted minimum approaches the baseline solution long after the gust has ceased.

We define the time constant τ_{slow} as the time after the gust ceases at which Dz_{min} falls to 0.05 (*i.e.* to 5% of its peak value), and compare it with the diffusive time constant proposed by VSN, given by

$$(19) \quad \tau_{\text{diff}} = z_{\text{min}}^2 / K_m.$$

As z_{min} in the above definition itself depends on K_m (and on time), τ_{diff} is not a simple function of K_m . For $z_{\text{min}} = 20$ cm and K_m equal to the standard value for air, the estimate for t_{diff} from (19) is 1600 s or 0.44 h.

To find out the relation between τ_{slow} and τ_{diff} , we again evaluate τ_{slow} from different simulations for three values of diffusivity differing from each other by a factor of 10. It can be seen from table II that τ_{slow} and τ_{diff} are of the same order for the corresponding values of K_m . (τ_{diff} was calculated using the value of z_{min} at 1 h, the initial instant of the gust.) Hence, it can be concluded that the approach to the base line solution occurs by diffusive relaxation.

In summary, when calm conditions are restored after a gust, the lifted minimum re-emerges as a result of a quick radiative adjustment over a time scale of the order of 10 s that increases as the ground emissivity moves closer to unity. But the eventual relaxation of the lifted minimum to the baseline solution occurs over a much longer time scale of the order of an hour, and is basically diffusive.

We wish to emphasize that although the focus here is on what may appear to be a

TABLE II. – *The slow time constant in gust episode.*

Diffusivity (m^2/s)	τ_{slow} (h)	τ_{diff} (h)
$0.1K_m$	1.75	1.71
K_m	2.25	1.83
$10K_m$	2.15	1.57

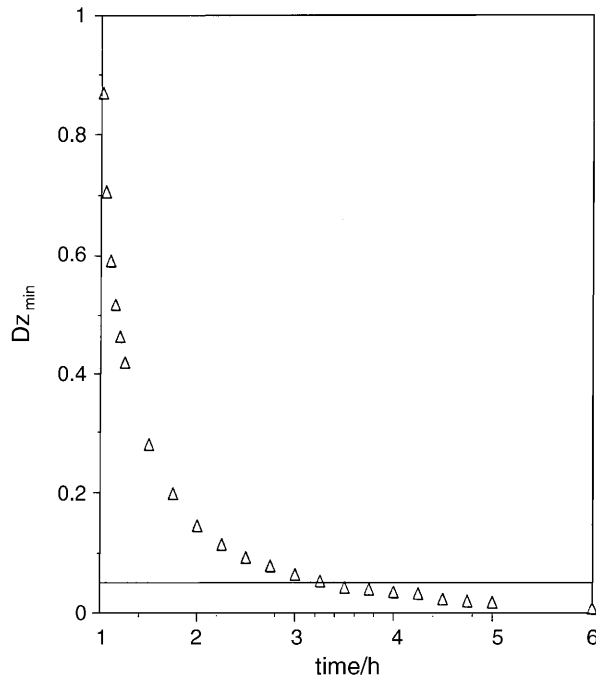


Fig. 13. – The evolution of the quantity Dz_{\min} for the baseline case with diffusivity equal to the standard value of air.

relatively singular phenomenon, the present effort, by showing how a canonical problem can be tackled, has wider implications for understanding nocturnal boundary layers. Apart from the results on nocturnal inversion considered in a companion paper, we may briefly mention the problem of the response of the atmospheric boundary layer to a total solar eclipse. An observational study made at Raichur, India in 1980 [33] identified three different time scales on which the response to the eclipse was expressed. Of these the first two are comparable to the time scales analysed here; in particular, it seems very likely that the many effects noted as occurring in times of the order of a minute are part of what we have termed here the quick radiative adjustment. The somewhat longer time scale could in part be the mark of the diffusive relaxation process (which becomes relevant because of the suppression of turbulence that occurs during the eclipse). These analogies are relevant as a total solar eclipse produces conditions similar to those expected at sunset, but on shorter time scales.

6. – Conclusions

The simulations reported in this paper throw much light on the time evolution of temperature distributions near ground on calm, clear nights. If the surface emissivity is below unity, a lifted temperature minimum tends to form shortly after nominal sunset. The nature of its further evolution during night, however, depends strongly on the ground cooling rate parameter β (which is a surrogate in the present approach for the inverse square root of the soil thermal diffusivity). If β is relatively low (a few degrees $\text{h}^{-1/2}$), the temperature minimum marks the top of a conduction layer whose thickness grows

in proportion to $t^{1/2}$, exactly as in the classical Rayleigh problem. If β is much higher (about $10 \text{ Kh}^{-1/2}$ or greater), the height of the lifted minimum at first rises, then reaches a maximum, and finally collapses. For moderate values of β the layer can achieve a nearly steady state. Thus the present work shows that the reports in the earlier literature can be reconciled, in that different types of behaviour of the lifted minimum are possible depending on surface properties at the site.

The dynamics of the distribution is further illuminated by its response to a turbulence episode. It is found that a gust quickly destroys the lifted minimum (over a time of the order of 20 s). After the cessation of the gust, however, evolution takes place on two disparate time scales; a fast process (over times of order 10–20 s) characterising a quick radiative adjustment (during which a lifted minimum re-emerges), and a slow process (times of order 10^3 s) characterising diffusive relaxation, during which the no-gust distribution is eventually attained again.

* * *

This work has been supported through a grant from the Department of Science & Technology. We are grateful to Prof. A. PRABHU for his valuable support and help in carrying out this project. The work reported here is a part of the M.Sc. thesis of SR, submitted to the Indian Institute of Science at the Department of Aerospace Engineering.

REFERENCES

- [1] LETTAU H. H., *Boundary Layer Meteorol.*, **17** (1979) 443.
- [2] RAMDAS L. A. and ATMANATHAN S., *Beit. Geophys.*, **37** (1932) 116.
- [3] VASUDEVA MURTHY A. S., SRINIVASAN J. and NARASIMHA R., *Philos. Trans. R. Soc. London*, **344** (1993) 183.
- [4] RASCHKE K., *Met. Rundschau*, **10** (1957) 1, English translation in Report 94 AS 2, 1957, Centre for Atmospheric Sciences, Indian Institute of Science, Bangalore, India.
- [5] GARRATT J. R., *The Atmospheric Boundary Layer* (Cambridge University Press) 1992.
- [6] GARRATT J. R., *J. Climate*, **8** (1995) 1360.
- [7] GEIGER R., *The Climate Near the Ground* (Harvard University Press, Cambridge, Mass.) 1965.
- [8] RAMDAS L. A., Tech. Note No. 21, India Met. Dept. (1945).
- [9] LAKE J. V., *Q. J. R. Meteorol. Soc.*, **82** (1956) 187.
- [10] OKE T. R., *Q. J. R. Meteorol. Soc.*, **96** (1970) 14.
- [11] NARASIMHA R., *Current Science*, **66** (1994) 16.
- [12] ZDUNKOWSKI W., *Beitr. Phys. Atmos.*, **39** (1966) 247.
- [13] LAKE J. V., *Q. J. R. Meteorol. Soc.*, **82** (1956) 530.
- [14] NARASIMHA R. and VASUDEVA MURTHY A. S., *Boundary-Layer Meteorol.*, **76** (1995) 307.
- [15] NARASIMHA R., in *Theoretical and Applied Mechanics, ICTAM 96*, edited by T. TATSUMI, E. WATANABE and T. KAMBE (Elsevier Science, Amsterdam) 1997, pp. 567-582.
- [16] LIOU K. -N., *An Introduction to Atmospheric Radiation* (Academic Press, New York) 1980.
- [17] RAMDAS L. A., *Arch. Met. Geophys. Bioklim.*, **3** (1951) 149.
- [18] RAMANATHAN K. R. and RAMDAS L. A., *Proc. Ind. Acad. Sci.*, **1** (1935) 822.
- [19] BROST R. A. and WYNGAARD J. C., *J. Atmos. Sci.*, **35** (1978) 1427.
- [20] CAUGHEY S. J., WYNGAARD J. C. and KAIMAL J. C., *J. Atmos. Sci.*, **36** (1979) 1041.
- [21] KUO H. L., *J. Atmos. Sci.*, **25** (1968) 682.
- [22] KONDO J., *J. Meteorol. Soc. Jpn.*, **9** (1971) 75.
- [23] ZILITENKEVICH, *AIAA J.*, **23** (1985) 938.

- [24] BUSINGER J. A., WYNGAARD J. C., IZUMI Y. and BRADLEY E. F., *J. Atmos. Sci.*, **28** (1971) 181.
- [25] LIOU K. -N. and OU S. -C., *J. Atmos. Sci.*, **40** (1983) 214.
- [26] GARRATT J. R. and BROST R. A., *J. Atmos. Sci.*, **38** (1981) 2730.
- [27] ZDUNKOWSKI W. and JOHNSON F. G., *J. Appl. Meteorol.*, **4** (1966) 371.
- [28] PALTRIDGE G. W. and PLATT C. M. R., *Radiative Processes in Meteorology and Climatology* (Elsevier Sci. Pub. Company, Amsterdam) 1976.
- [29] BRUNT D., *Physical and Dynamical Meteorology*, 2nd edition (Cambridge University Press) 1941.
- [30] KAIMAL J. C. and FINNIGAN J. J., *Atmospheric Boundary Layer Flows* (Oxford University Press) 1994.
- [31] VASUDEVA MURTHY A. S., SRINIVASAN J. and NARASIMHA N., Report 91 AS 1, 1991, Centre for Atmospheric Sciences, Indian Institute of Science, Bangalore.
- [32] CARSLAW H. S. and JAEGAR J. C., *Conduction of Heat in Solids* (Oxford University Press) 1959.
- [33] NARASIMHA R., PRABHU A., NARAHARI RAO K. and PRASAD C. R., *Proc. Ind. Natl. Acad. Sci. A*, **48** (1982) 175.